

Construction of density-dependent α -nucleon interaction to describe α -nucleus scattering

Takenori Furumoto^{1,*}, Kohsuke Tsubakihara², Shuichiro Ebata³, and Wataru Horiuchi^{4,5,6,7}

¹College of Education, Yokohama National University, Yokohama 240-8501, Japan

²National Institute of Technology, Asahikawa College, Asahikawa 071-8142, Japan

³Graduate School of Science and Engineering, Saitama University, Saitama 338-8570, Japan

⁴Department of Physics, Osaka Metropolitan University, Osaka 558-8585, Japan

⁵Nambu Yoichiro Institute of Theoretical and Experimental Physics (NITEP), Osaka Metropolitan University, Osaka 558-8585, Japan

⁶RIKEN Nishina Center, Wako 351-0198, Japan

⁷Department of Physics, Hokkaido University, Sapporo 060-0810, Japan

Abstract. We provide a global density-dependent α -nucleon (DD- αN) interaction to construct the α -nucleus optical potential in a wide range of incident energies. The α -nucleus potential based on the folding model with the present DD- αN interaction reproduces the experimental data up to backward angles using the point-nucleon density obtained by the mean-field model. The present DD- αN interaction is based on the phenomenological optical potential to reproduce the $p + {}^4\text{He}$ elastic scattering at the incident energies at 12.04–1000 MeV. Namely, the α -nucleon system is considered an elementary process. The density dependence (medium effect) of the DD- αN interaction is phenomenologically added to reproduce the α elastic scatterings by the ${}^{16}\text{O}$, ${}^{40}\text{Ca}$, ${}^{58}\text{Ni}$, ${}^{90}\text{Zr}$ and ${}^{208}\text{Pb}$ targets at $E/A = 10\text{--}342.5$ MeV. The total reaction cross sections are also compared with the experimental data.

1 Introduction

A global description of the optical potential has been attempted from the microscopic viewpoint. The nucleus-nucleus potential has often been constructed from the nucleon-nucleon interaction using the densities of the interacting nuclei in the double-folding model. Such efforts are presented in Refs. [1–8]. The α -nucleus potential has also been constructed in the double-folding model. Plenty of the microscopic α -nucleus potentials are proposed in the folding model approach [9–15]. However, these prescriptions are inconsistent in constructing the α -nucleus folding potential. In addition, α -nucleus potential is heterogeneous in comparison with the nucleus-nucleus potential for heavy-ion scattering. Here, we clarify the problem for the α scattering with results by the CDM3Y6 [11] and JLM [16] interactions.

The folding potentials with the CDM3Y6 and JLM interactions have the same problem for the α -nucleus system. The double-folding model potentials with the CDM3Y6 and JLM interactions need to introduce renormalization factors in reproducing the data, which are often defined as

$$U = N_R V_{\text{CDM3Y6}} + iW_{\text{phenome.}} \quad (1)$$

*e-mail: furumoto-takenori-py@ynu.ac.jp

and

$$U = N_R V_{\text{JLM}} + iN_I W_{\text{JLM}}, \quad (2)$$

for the CDM3Y6 and JLM interactions, respectively. Here, V_{CDM3Y6} is the folding model potential with the CDM3Y6 interaction. V_{JLM} and W_{JLM} are the real and imaginary parts of the folding model potential with the JLM interaction, respectively. $W_{\text{phenome.}}$ is the phenomenological imaginary potential. The N_R and N_I are the real and imaginary parts of the renormalization factor, respectively. We compare the real part of the renormalization factor (N_R) for the α -nucleus system with that for the nucleus-nucleus ones. Here, the nucleus-nucleus system means heavy-ion scattering. Figure 1 shows the renormalization factors of

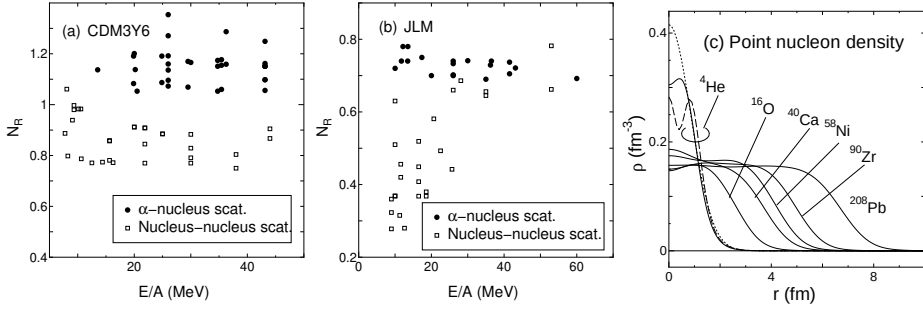


Figure 1. N_R with (a) the CDM3Y6 interaction and (b) the JLM interaction. E/A is the incident energy per nucleon. The values are taken from [2, 3, 9, 11–13, 17–19]. (c) Density distribution of point nucleon matter for ${}^4\text{He}$, ${}^{16}\text{O}$, ${}^{40}\text{Ca}$, ${}^{58}\text{Ni}$, ${}^{90}\text{Zr}$ and ${}^{208}\text{Pb}$. The density distributions are taken from Refs. [13, 20–22].

the real part with (a) the CDM3Y6 interaction and (b) the JLM interaction. The filled circles are N_R of the α -nucleus system. The open squares are N_R of the nucleus-nucleus system. We see that the behavior of the renormalization factors for the α -nucleus system is different from that for the nucleus-nucleus system. This problem occurs when prescriptions in the α -nucleus and the nucleus-nucleus systems are treated in the same manner.

We construct a density-dependent α -nucleon (DD- αN) interaction to address this problem. In general, the effective nucleon-nucleon interaction for the nuclear reaction is not optimized to the ${}^4\text{He}$ nucleus. Almost all effective nucleon-nucleon interactions for the nuclear reaction take into account the property in the infinite nuclear matter. However, it should be noted that the α particle is far from the condition of the infinite nuclear matter. As shown in Fig. 1 (c), the inner part of the density for the α particle is well known to be higher than the saturation density which is adopted as the saturation point in the nuclear matter. In addition, the binding energy of the α particle is not obtained by the mass formula which leads to the saturation energy in the nuclear matter. Therefore, rather than the nucleon-nucleon interaction, it is reasonable to consider the alpha-nucleon interaction as the elementary process underlying the α -nucleus scattering. The density dependence of the α -nucleon interaction is phenomenologically fixed to reproduce the experimental data. This density dependence is considered to express the medium effect. Here, we remark on some pioneering works for the DD- αN interactions [10, 23, 24]. The DD- αN interactions have adjustable parameters to reproduce the α -nucleus scattering. However, they are not designed to describe the $p + {}^4\text{He}$ system. This paper proposes a new DD- αN interaction that reproduces also the $p + {}^4\text{He}$ elastic scattering to construct the α -nucleus potential.

In this paper, we first explain the theoretical framework in Sec. 2. The $p + {}^4\text{He}$ optical potential and the functional form of the DD- αN interaction are explained. In Sec. 3, first, the

results of the $p + {}^4\text{He}$ elastic scattering are presented. Then, we show the results of the present folding model calculation for the α -nucleus elastic scattering for ${}^{16}\text{O}$, ${}^{40}\text{Ca}$, ${}^{58}\text{Ni}$, ${}^{90}\text{Zr}$ and ${}^{208}\text{Pb}$. The total reaction cross sections are also calculated and compared with experimental data. Lastly, we summarize this work in Sec. 4.

2 Formalism

We construct the α -nucleus potential with the DD- αN interaction and point-nucleon density obtained by the Hartree Fock +BCS (HF+BCS) calculation [22] in the folding procedure.

2.1 $p + {}^4\text{He}$ potential

We first construct the $p + {}^4\text{He}$ potential in the phenomenological optical model. The optical model potential (U) is designed as

$$U(s, E/A) = f(s; V_0, r_0, a_0) + f(s; V_1, r_1, a_1) + if(s; W, r_W, a_W) + \frac{\lambda_\pi^2}{r_{\text{SO}} A_\alpha^{1/3}} \frac{d}{ds} f(s; V_{\text{SO}}, r_{\text{SO}}, a_{\text{SO}}) \boldsymbol{\ell} \cdot \boldsymbol{\sigma} \quad (3)$$

with

$$f(s; V, r, a) = -\frac{V}{1 + \exp\left(\frac{s - rA_\alpha^{1/3}}{a}\right)}, \quad (4)$$

where s is the distance between the proton and the ${}^4\text{He}$ nucleus. $A_\alpha = 4$. E/A is the incident energy per nucleon. The real part of the potential is designed by double Woods-Saxon (WS) type potential to express the wine-bottle shape and repulsive potential at high energy [25–27]. The imaginary part is a standard WS type. The spin-orbit potential has a standard form called the derivative WS type. Here, $\lambda_\pi^2 = 2.0 \text{ fm}^2$. The parameters ($V_0, r_0, a_0, V_1, r_1, a_1, W, r_W, a_W, V_{\text{SO}}, r_{\text{SO}}$ and a_{SO}) are fixed to reproduce the experimental data for each incident energy. We note that the notation of E/A in parameters is omitted for simplicity. Their specific functions and parameters will be presented later.

2.2 Global density-dependent α -nucleon interaction

Next, we introduce the present DD- αN interaction. The present DD- αN interaction ($U_{\text{DD-}\alpha N}$) has a form

$$U_{\text{DD-}\alpha N}(s, \rho, E/A) = f(s; V_0, r_0, a_0)g_0(\rho, E/A) + f(s; V_1, r_1, a_1)g_1(\rho) + if(s; W, r_W, a_W)g_W(\rho), \quad (5)$$

where ρ is the input density, which determines a medium effect. In addition, g_0 , g_1 and g_W are the density-dependent functions for the real and imaginary parts, respectively, which are explicitly written as

$$g_0(\rho, E/A) = \exp(-\beta_0 \rho), \quad (6)$$

$$g_1(\rho) = 1 + \beta_1 \rho, \quad (7)$$

$$g_W(\rho) = \exp(-\beta_W \rho), \quad (8)$$

where β_0 , β_1 and β_W are globally fixed to reproduce the α -nucleus scattering data. Here, we note that $\beta_0 = \beta_0(E/A)$. The energy dependence of β_0 will be introduced later. These parameters are fixed to reproduce the α -nucleus scattering. The core part (Eq. (7)) is taken

from Ref. [10]. Their specific values (β_0 , β_1 and β_w) will be presented in the following section.

With this DD- α interaction, we construct the α -nucleus potential in the same manner as Refs. [10, 23, 24, 28]. We apply the point-nucleon density of ^{16}O , ^{40}Ca , ^{58}Ni , ^{90}Zr and ^{208}Pb obtained from the mean-field model (HF+BCS). The detail of the derivation is given in Refs. [22, 29].

3 Results and Discussion

We show the calculated results in this section. We first construct the bare αN interaction which is the $p + ^4\text{He}$ optical potential. After that, we compute the α elastic scattering cross sections by applying the DD- αN interaction. The total reaction cross sections are also evaluated. Here, we apply the standard Coulomb potential of a uniform charge. We use the radius of uniform charge, $R_C = 1.3 \cdot 4^{1/3}$ fm for $p + ^4\text{He}$ system and $R_C = 1.3(4^{1/3} + A^{1/3})$ fm for $\alpha + \text{nucleus}$ system, respectively. A is the mass number of the target nucleus. Relativistic kinematics is used to compute the cross sections.

We note that the imaginary part of the folding potential is based on the $p + ^4\text{He}$ reaction even if the density dependence is introduced. However, the imaginary part of the α -nucleus potential also includes the contribution from the target nucleus. Thus, the imaginary part of the resulting α -nucleus potential with the present DD- αN interaction can be different. Therefore, we introduce the renormalization factor to the imaginary part as

$$U_{\alpha A}(R; E/A) = V_{\alpha A}(R; E/A) + iW_{\alpha A}(R; E/A) \quad (9)$$

$$\rightarrow V_{\alpha A}(R; E/A) + iN_I W_{\alpha A}(R; E/A), \quad (10)$$

where $V_{\alpha A}(R; E/A)$ and $W_{\alpha A}(R; E/A)$ are the real and imaginary parts of the constructed α -nucleus potential with the present DD- αN interaction.

3.1 $p + ^4\text{He}$ elastic scattering

With the form of the optical potential of Eq. (3), we calculate the $p + ^4\text{He}$ elastic cross section. The incident energy (E/A) dependent parameters are fixed to reproduce the $p + ^4\text{He}$ elastic scattering, which are listed in Table 1.

Table 1. Parameters of the $p + ^4\text{He}$ optical potential.

V_0 (MeV)	r_0 (fm)	a_0 (fm)
$-2.31(E/A)^{1/2} + 78.5$	$0.00153(E/A) - 0.0798(E/A)^{1/2} + 1.5$	$0.0269(E/A)^{1/2} + 0.262$
V_1 (MeV)	r_1 (fm)	a_1 (fm)
$-3.71(E/A)^{1/2} + 14.6$	0.8	$0.0044(E/A)^{1/2} + 0.19$
W (MeV)	r_w (fm)	a_w (fm)
$1.6(E/A)^{1/2} - 0.51$	$-0.0116(E/A)^{1/2} + 1.18$	0.5
V_{SO} (MeV)	r_{SO} (fm)	a_{SO} (fm)
$-0.423(E/A)^{1/2} + 12$	0.7	0.3

Figure 2 shows the elastic cross sections of the $p + ^4\text{He}$ system at 12.04–1000 MeV. The solid curves are the results obtained by the present work. It is known that the cross sections at the backward angles for the $p + ^4\text{He}$ system cannot be fully described by the normal one-body potential. Other reaction mechanisms such as knock-on type exchange scattering are

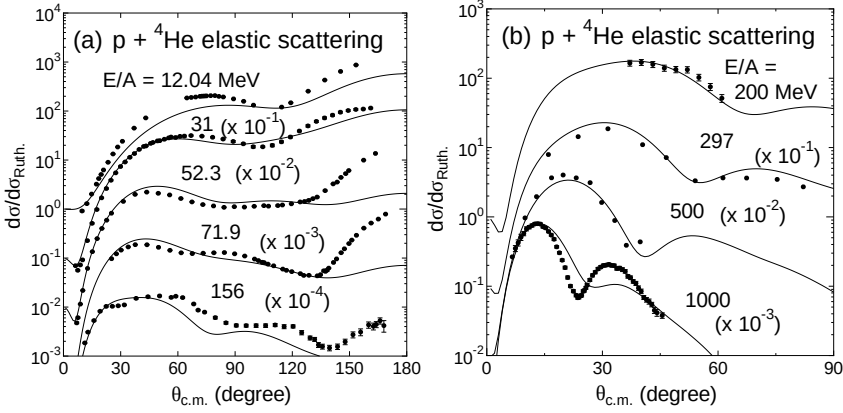


Figure 2. Elastic cross sections of the $p + {}^4\text{He}$ system at (a) $E/A = 12.04\text{--}156$ MeV and (b) $E/A = 200\text{--}1000$ MeV. The solid curves are the results obtained by the present work. The experimental data are taken from [30–39].

needed to describe these backward cross sections. We confirm that the $p + {}^4\text{He}$ elastic cross sections are well reproduced by the present DD- αN interaction. Next, we apply this $p + {}^4\text{He}$ potential to the folding model to describe the α elastic scattering.

3.2 α -nucleus elastic scattering

In this subsection, we show the results of the α -nucleus elastic scattering. We choose the ${}^{16}\text{O}$, ${}^{40}\text{Ca}$, ${}^{58}\text{Ni}$, ${}^{90}\text{Zr}$ and ${}^{208}\text{Pb}$ nuclei as a target, in which plenty of experimental data for the α -nucleus elastic scattering exist.

First, we show the parameters fixed in the present paper. The parameters introduced in Eqs. (6), (7) and (8) are shown in Table 2. They are fixed to reproduce the experimental data. In the fitting procedure, we find that β_0 has an energy dependence, which implies the medium effect is not unique for all incident energies.

Table 2. Parameters of the density-dependent part of the present DD- αN interaction.

β_0 (fm ³)	β_1 (fm ³)	β_W (fm ³)
$6.56 \exp\left(-\frac{(E/A)^2}{65^2}\right) + 2.3$	4.3	9.8

Figure 3 shows the results of (a) the $\alpha + {}^{16}\text{O}$ elastic scattering at $E/A = 12\text{--}100$ MeV, (b) the $\alpha + {}^{40}\text{Ca}$ elastic scattering at $E/A = 10.5\text{--}342.5$ MeV and (c) the $\alpha + {}^{58}\text{Ni}$ elastic scattering at $E/A = 13.1\text{--}174.8$ MeV, (d) the $\alpha + {}^{90}\text{Zr}$ elastic scattering at $E/A = 10\text{--}96.5$ MeV and (e) the $\alpha + {}^{208}\text{Pb}$ elastic scattering at $E/A = 26\text{--}174.8$ MeV. The present DD- αN interaction reproduces the data up to backward angles well with the appropriate N_I value. The N_I values are shown in Fig. 4 (a).

Figure 4 (b) shows the results of the total reaction cross section for the incident α particle for the ${}^{16}\text{O}$, ${}^{40}\text{Ca}$, ${}^{58}\text{Ni}$, ${}^{90}\text{Zr}$, and ${}^{208}\text{Pb}$ targets. The total reaction cross sections are well reproduced, even though they are not used in the fitting procedure. The density-dependent parameters obtained in the present work are considered to be global. Namely, the present DD- αN interaction can be applied to other systems only with one free parameter, the renor-

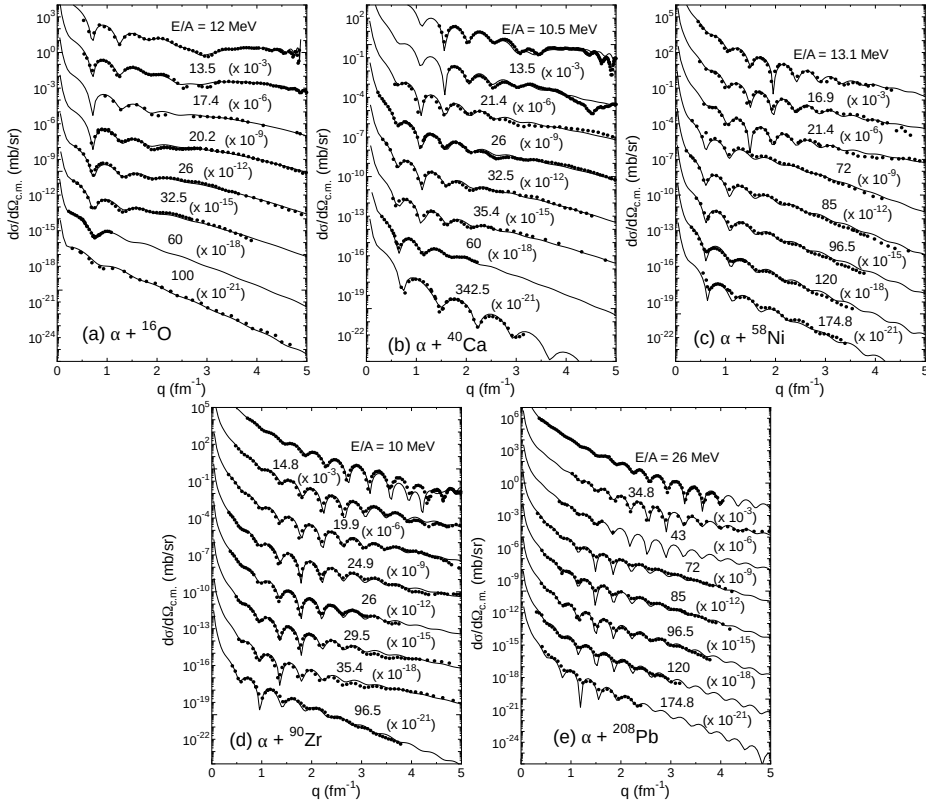


Figure 3. Elastic cross sections of (a) $\alpha + {}^{16}\text{O}$ system at $E/A = 12\text{--}100$ MeV, (b) $\alpha + {}^{40}\text{Ca}$ system at $E/A = 10.5\text{--}342.5$ MeV, (c) $\alpha + {}^{58}\text{Ni}$ system at $E/A = 13.1\text{--}174.8$ MeV, (d) $\alpha + {}^{90}\text{Zr}$ system at $E/A = 10\text{--}96.5$ MeV and (e) $\alpha + {}^{208}\text{Pb}$ system at $E/A = 26\text{--}174.8$ MeV. The solid curves denote the present results. The experimental data are taken from [30, 40–57].

malization factor of the imaginary part of the α -nucleus potential, which can be fixed if the total reaction cross section exists.

4 Summary

We have developed a global DD- αN interaction to describe the α -nucleus elastic scattering. The present DD- αN interaction is constructed based on a reliable $p + {}^4\text{He}$ potential, which reproduces the $p + {}^4\text{He}$ elastic scattering cross section data. The density-dependent part of the DD- αN interaction is phenomenologically fixed to reproduce the α -nucleus elastic scattering. We show the α -nucleus elastic scattering cross sections with ${}^{16}\text{O}$, ${}^{40}\text{Ca}$, ${}^{58}\text{Ni}$, ${}^{90}\text{Zr}$ and ${}^{208}\text{Pb}$ targets and confirm that the present DD- αN interaction well reproduces the data up to backward angles in a wide range of incident energies $E/A = 10\text{--}342.5$ MeV only with one free parameter. We see that the total reaction cross section can be used to fix it. All the details will be reported elsewhere soon [28].

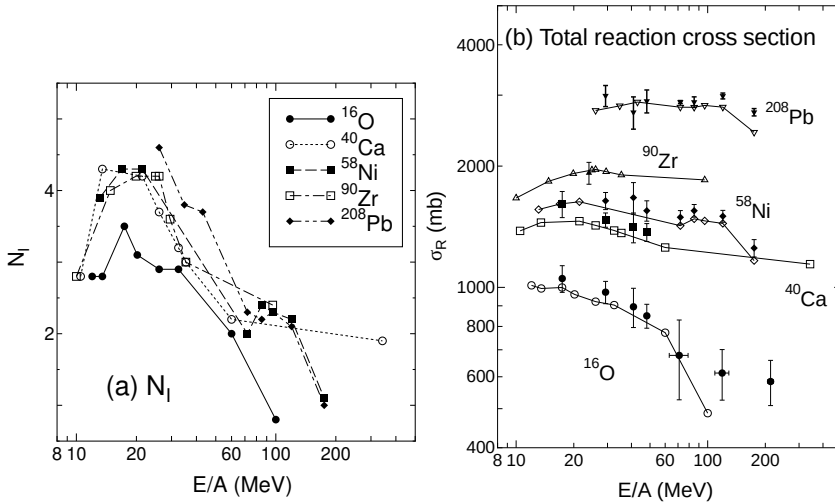


Figure 4. (a) Renormalization factor for the imaginary part used in this paper and (b) Total reaction cross section for the incident α particle. The filled mark with the error bar is the experimental data. The open symbols connected with a solid line are the present results. The experimental data are taken from Refs. [53, 58–60].

Acknowledgment

The authors would like to acknowledge Professor Y. Iseri for providing the (unpublished) ALPS computer code to search the optical model potential. This work was supported by the Japan Society for the Promotion of Science (JSPS) KAKENHI Grant Numbers JP18K03635, JP20K03943 JP20K03944 and JP22H01214.

References

- [1] G. R. Satchler and W. G. Love, Phys. Rep. **55**, 184 (1979)
- [2] Dao T. Khoa and G. R. Satchler, Nucl. Phys. **A668**, 3 (2000)
- [3] Dao T. Khoa et al., Nucl. Phys. **A759**, 3 (2005)
- [4] T. Furumoto, Y. Sakuragi and Y. Yamamoto, Phys. Rev. C **80**, 044614 (2009)
- [5] T. Furumoto and Y. Sakuragi, Phys. Rev. C **87**, 014618 (2013)
- [6] T. Furumoto, Y. Sakuragi and Y. Yamamoto, Phys. Rev. C **94**, 044620 (2016)
- [7] T. Furumoto, T. Suhara and N. Itagaki, Phys. Rev. C **97**, 044602 (2018)
- [8] W. Horiuchi and T. Furumoto, Nucl. Phys. **A1011**, 122204 (2021)
- [9] F. Carstoiu and M. Lassau, Nucl. Phys. **A597**, 269 (1996)
- [10] G. R. Satchler and Dao T. Khoa, Phys. Rev. C **55**, 285 (1997)
- [11] Dao T. Khoa, G. R. Satchler and W. von Oertzen, Phys. Rev. C **56**, 954 (1997)
- [12] Dao T. Khoa, Phys. Rev. C **63**, 034007 (2001)
- [13] T. Furumoto and Y. Sakuragi, Phys. Rev. C **74**, 034606 (2006)
- [14] Dao T. Khoa et al., J. Phys. G: Nucl. Part. Phys. **34**, R111 (2007)
- [15] K. Egashira et al., Phys. Rev. C **89**, 064611 (2014)
- [16] J. P. Jeukenne, A. Lejeune, and C. Mahaux, Phys. Rev. C **16**, 80 (1977)
- [17] Dao T. Khoa et al., Nucl. Phys. **A672**, 387 (2000)

- [18] A. A. Ogloblin et al., Phys. Rev. C **62**, 044601 (2000)
- [19] L. Trache et al., Phys. Rev. C **61**, 024612 (2000)
- [20] M. Takashina and Y. Sakuragi, Phys. Rev. C **74**, 054606 (2006)
- [21] W. Horiuchi and Y. Suzuki, Phys. Rev. C **87**, 034001 (2013)
- [22] S. Ebata et al., Phys. Rev. C **82**, 034306 (2010)
- [23] F. E. Bertrand, et al., Phys. Rev. C **22**, 1832 (1980)
- [24] A. Kolomiets, O. Pochivalov, and S. Shlomo, Phys. Rev. C **61**, 034312 (2000)
- [25] S. Hama et al., Phys. Rev. C **41**, 2737 (1990)
- [26] N. V. Sen et al., Nucl. Phys. **A464**, 717 (1987)
- [27] T. Furumoto, Y. Sakuragi, and Y. Yamamoto, Phys. Rev. C **82**, 044612 (2010)
- [28] T. Furumoto, K. Tsubakihara, S. Ebata, and W. Horiuchi, accepted for publication in Prog. Theor. Exp. Phys (2023).
- [29] T. Furumoto, K. Tsubakihara, S. Ebata, and W. Horiuchi, Phys. Rev. C **99**, 034605 (2019)
- [30] <https://www.jcprg.org/exfor/>
- [31] J. Sanada, Conf. Nucl. Forces and Few-Nucleon Probl. 663 (1959)
- [32] S. M. Bunch, H. H. Forster, and C. C. Kim, Nucl. Phys. **53**, 241 (1964)
- [33] K. Imai et al., Nucl. Phys. **A325**, 397 (1979)
- [34] S. Burzynski et al., Phys. Rev. C **39**, 56 (1989)
- [35] V. Comparat et al., Phys. Rev. C **12**, 251 (1975)
- [36] S. Chebotaryov et al., Prog. Theor. Exper. Phys. **2018**, 053D01 (2018)
- [37] M. Yoshimura et al., Phys. Rev. C **63**, 034618 (2001)
- [38] S. M. Sterbenz et al., Phys. Rev. C **45**, 2578 (1992)
- [39] G. D. Alkhazov et al., Soviet Journal of Nuclear Physics **41**, 357 (1985)
- [40] N. Burtebayev et al., International Journal of Modern Physics E **26**, 1750018 (2017)
- [41] H. Abele et al., Z. Phys. **A326**, 373 (1987)
- [42] F. Michel et al., Phys. Rev. C **28**, 1904 (1983)
- [43] G. Hauser et al., Nucl. Phys. **A128**, 81 (1969)
- [44] S. Adachi et al., Phys. Rev. C **97**, 014601 (2018)
- [45] Y.-W. Lui, H. L. Clark, and D. H. Youngblood, Phys. Rev. C **64**, 064308 (2001)
- [46] T. Wakasa et al., Phys. Lett. **B653**, 173 (2007)
- [47] H. P. Gubler et al., Nucl. Phys. **A351**, 29 (1981)
- [48] H. H. Chang Nucl. Phys. **A270**, 413 (1976)
- [49] H. J. Gils et al., Phys. Rev. C **21**, 1239 (1980)
- [50] D. A. Goldberg, S. M. Smith, and G. F. Burdzik, Phys. Rev. C **10**, 1362 (1974)
- [51] D. H. Youngblood, Y.-W. Lui, and H. L. Clark, Phys. Rev. C **55**, 2811 (1997)
- [52] G. D. Alkhazov et al., Nucl. Phys. **A280**, 365 (1977)
- [53] B. Bonin et al., Nucl. Phys. **A445**, 381 (1985)
- [54] M. Uchida et al., Phys. Rev. C **69**, 051301(R) (2004)
- [55] L. W. Put and A. M. J. Paans, Nucl. Phys. **A291**, 93 (1977)
- [56] D. A. Goldberg et al., Phys. Rev. C **7**, 1938 (1973)
- [57] H. P. Morsch Phys. Rev. C **22**, 489 (1980)
- [58] A. Ingemarsson et al., Nucl. Phys. **A676**, 3 (2000)
- [59] F. Horst et al., Phys. Rev. C **99**, 014603 (2019)
- [60] A. D. Duysebaev et al., Physics of Atomic Nuclei **66**, 599 (2003)